AN OPTIMIZED DESIGN METHOD OF GNSS EXTERNAL DEFORMATION MONITORING SCHEME FOR DAM PROJECT IN ALPINE CANYON AREA

LI ZUFENG AND ZHOU HENG
Northwest Engineering Corporation Limited, Xi'an, Shaanxi, China

ZHAO QINGZHI
College of Geomatics, Xi'an University of Science and Technology, Xi'an, Shaanxi, China

ZHAO YANHUA
Gansu Agricultural University, Lanzhou, Gansu, China

ABSTRACT

When monitoring the external deformation for dams in alpine valleys using the Global Navigation Satellite System (GNSS) technique, some shortcomings, such as the small number of satellites visible and the low intensity of constellation space geometry structure, are inevitable. Therefore, how to monitor the dam project precisely under the above specific conditions using GNSS technique is a difficult problem. This study established the satellite boundary constraints by quantifying the terrain and obstacle information around GNSS monitoring stations, and developed a method to evaluate the accuracy of single GNSS station based on the satellite visibility and satellite distribution during monitoring period. At the same time, the double-difference equation and error equation of GNSS observation are established with the constraints of visual satellite. The relative positioning accuracy factor of baseline is determined using the correlation coefficients matrix of the unknown parameters, and the synchronous observation combination of GNSS monitoring points is determined accordingly. The observation accuracy of synchronous loop is estimated according to the selected network conditions and the corresponding precision factor of observation period, and thus the synchronous GNSS monitoring stations and periods are determined. Finally, the GNSS network is constructed based on multiple synchronous loops, and the accuracy of the GNSS network can be estimated by the variance matrix estimation method of the baseline vector. Experimental results show that the accuracy of the proposed control network is highly consistent with the actual satellite status, which has important research significance and application value for the development of GNSS observation plan in the environment of Alpine Canyon and urban area.

1. INTRODUCTION

Existing satellite ephemeris forecasts do not effectively take into account station occlusion conditions (Hao et al. 2008, Hao et al. 2001, Li & Bian 2009, Yao et al. 2012, Wang et al. 2007, Du et al. 2009, Shi et al. 2004, Niu & Lai 1998). Generally, satellite visibility is judged by setting a fixed altitude angle such as 10° or 15° or manually setting a general satellite screening condition. But in fact, because of the barrier occlusion, such as the high mountain canyon area, the environmental impact of urban buildings, the actual satellite signals can be received will have a large gap. When the cutoff height angle E is 30° (Li et al. 2010). The time of sight of four or more GPS satellites is 90% of the total number of days. At 40°C, the time of sight of four or more GPS satellites is 47% of the total number of days. In the high mountain canyon area, the height angle occlusion of more than 30° is often encountered, and the accuracy of the ephemeris prediction according to the general method has a great error. Therefore, it is necessary to study the satellite occlusion boundary condition establishment method for measuring target points, and the ephemeris prediction, baseline evaluation, control network accuracy estimation method based on satellite occlusion boundary condition, in order to carry out more effective ephemeris prediction, obtain more accurate forecast precision factor, and then study the prediction method of baseline relative precision factor to further optimize the shape and observation scheme of GNSS measurement control network.

This is Research One of the aim is to provide an ephemeris prediction method that takes into account the satellite occlusion condition.

Another objective of this study is Provision of a GNSS measurement Control network accuracy estimation method to solve the existing estimation method Effective Considering the occlusion condition of the station, the influence on the baseline accuracy estimation makes the accuracy of the control network more accurately reflect the actual measurement accuracy.

2. ESTABLISHMENT OF CONSTRAINT CONDITIONS AND SCREENING OF VISIBLE SATELLITES FOR SHELTER BOUNDARIES OF STATION SATELLITES

2.1 Determination of the occlusion altitude angle of the target point satellite based on the central coordinates of the station

Based on topographic map, digital elevation model (dem) or other digital geographic information products with elevation attributes to measure the height angle of target point satellite, this study uses digital line drawing and dem model to measure the measurement respectively. the basic principles are as follows.

First of all, determine the target point coordinates, take the target point as the center to establish the station center coordinate system, take the target point as the center from the north direction to start clockwise each separation certain angle (recommended to use 5°) to measure a section, the section measurement length is determined according to the actual situation, according to our measured effect comparison, generally should not be less than 2 km, according to the measured section characteristics point, calculate the corresponding direction of the maximum occlusion angle, sequential measurement of each direction, get the target point corresponding to each direction of the occlusion height angle E_i.

Let the section line characteristic point measure n points, the height angle corresponding to each characteristic point for E_i^n:

$$E_i^n = arctan\left(\frac{H_i - H_0}{D_i}\right) \tag{1}$$

$D_i\ H_i\ H_0$ of which for the plane distance from the feature point of the section to the center of the station, for the elevation of the feature point of the section and for the elevation of the target point, the angle of occlusion height corresponding to each direction of the target point for E_i:

$$E_i = max[E_i^n] \tag{2}$$

The height angle of GNSS is generally expressed in the form of station center coordinate, so it is necessary to convert it to station center coordinate form when using topographic map and dem model data for height angle measurement.

Under the influence of the curvature of the earth, the formulas for calculating the influence of height difference are as follows:

$$\Delta H = \sqrt{(D^2 + R^2)} - R = \frac{S^2}{2R} \tag{3}$$

D when it is 2 km and 3 km, its effect on height difference is 0.31 m and 0.71 m. Therefore, the influence can be neglected in the general height angular measurement process, when there is a higher requirement to consider its influence, the formula for calculating the height angle of the characteristic point becomes E_i^n:

$$E_i^n = arctan\left(\frac{2RH_i - D_i^2 - 2RH_0}{2RD_i}\right) \tag{4}$$

The height angle of each direction can be measured in turn, and then the height angle measurement of single station can be completed.

The height angle measured by a single station is as follows:

$$\begin{cases} Po\ int\ \ name \\ A_1, E_1 \\ A_2, E_2 \\ \cdots \quad \cdots \\ A_i, E_i \\ \cdots \quad \cdots \\ A_n, E_n \end{cases} \tag{5}$$

2.2 Calculation of Satellite Height Angle and Azimuth Angle in Central Coordinate System

Analytic broadcast ephemeris is the basis of GNSS ephemeris prediction and precision evaluation, and is the precondition of satellite position calculation. By calculating the average angular velocity of the satellite motion, the average point angle of the observation moment, the near point angle, the true near point angle, the rising intersection angle distance and the perturbation correction term, the position of the satellite in the orbit plane coordinate system is calculated. Finally, the position of the satellite in the instantaneous earth coordinate system and the position in the protocol earth coordinate system are obtained by coordinate transformation. (Hao et al. 2001, Li & Bian 2009, Yao et al. 2012, Wang et al. 2007, Du et al. 2009, Shi et al. 2004, Niu & Lai 1998, Li et al. 2010, Li Z.F. 2010, Shi & Zhang 2000, Cao et al. 2013) and then converted into a central coordinate with the measuring station as the origin, and then obtained the satellite's height angle and azimuth angle.

The coordinates of the satellite in the center-of-station rectangular coordinate system are:

$$\begin{pmatrix} X_R^S \\ Y_R^S \\ Z_R^S \end{pmatrix} = H \begin{pmatrix} \Delta X_{RS} \\ \Delta Y_{RS} \\ \Delta Z_{RS} \end{pmatrix} \tag{6}$$

In the formula:

$$\begin{pmatrix} \Delta X_{RS} \\ \Delta Y_{RS} \\ \Delta Z_{RS} \end{pmatrix} = \begin{pmatrix} X_S \\ Y_S \\ Z_S \end{pmatrix} - \begin{pmatrix} X_R \\ Y_R \\ Z_R \end{pmatrix} \tag{7}$$

$\begin{bmatrix} X_R & Y_R & Z_R \end{bmatrix}^T$ for the station space coordinates.

$$H = \begin{bmatrix} -\sin B \cos L & -\sin B \sin L & \cos B \\ -\sin L & \cos L & 0 \\ \cos B \cos L & \cos B \sin L & \sin B \end{bmatrix} \tag{8}$$

Among them, B and L are the geodetic longitude and latitude of the station respectively.

Satellite altitude angle for e:

$$e = \arctan \frac{Z_R^S}{\sqrt{(X_R^S)^2 + (Y_R^S)^2}} \tag{9}$$

Azimuth of the satellite for A:

$$\begin{pmatrix} m \\ n \end{pmatrix} = \begin{pmatrix} -\sin B \cos L & \sin B \sin L & \cos B \\ -\sin L & \cos L & 0 \end{pmatrix} \begin{pmatrix} \Delta X_{RS} \\ \Delta Y_{RS} \\ \Delta Z_{RS} \end{pmatrix} \tag{10}$$

$$A = \arctan \frac{n}{m} \tag{11}$$

2.3 Station-based visible satellite screening

After obtaining the satellite altitude angle and azimuth angle at the selected measuring time, the target point visible satellite information can be obtained by calculating the measurement point occlusion height angle determined by the model according to formula (5), and then the filter screening of the obstacle occluded satellite can be realized. The calculation process is as follows:

The two adjacent occlusion height angles are known as: $(A_{i-1}\ ,\ E_{i-1})$, $(A_{i+1}\ ,\ E_{i+1})$, Solve the occlusion height angle here by linear interpolation:

$$E = aA + b \tag{12}$$

$(A_{i-1}\ ,\ E_{i-1})$, $(A_{i+1}\ ,\ E_{i+1})$, a, b, A_i you can find the parameters by substituting the above formula. The satellite azimuth angle of the specified time is substituted into the upper formula, and the height occlusion angle of the corresponding direction is obtained as follows:

$$E_i = aA_i + b \tag{13}$$

Compare the altitude angle of the satellite at the selected moment and occlusion altitude angle to judge the visibility of the observation satellite e E_i.

$e > E_i$ If so, the satellite will be retained or eliminated.

For the occlusion condition of the approximate linear change, the height angle interpolation can use I (set the number of occlusion height angle is n, I ⩽ n) to fit the fixed point height angle:

$$E = a_0 + a_1 A + a_2 A^2 + \ldots + a_n A^n \tag{14}$$

Thus the satellite condition of the obstacle is filtered one by one to determine the visibility of the satellite.

3. TARGET POINT DOP VALUE EVALUATION BASED ON THE CONSTRAINT CONDITIONS OF SATELLITE OCCLUSION BOUNDARY

Based on the above satellite visibility analysis method, the geometric precision factor DOP value can be further calculated, and the ephemeris prediction can be obtained. Follow the following steps:

Based on the state matrix of the satellite group obtained by the above satellite visibility method, the DOP value is calculated by using the direction cosine method, that is, the direction cosine calculation of the satellite constellation. The calculated DOP values include GDOP, PDOP, HDOP, VDOP and TDOP values. The technical routes are as follows:

The point observation accuracy information is obtained by using the station coordinates and satellite coordinates for the calculation of the DOP values (GDOP, PDOP, HDOP, VDOP and TDOP values) between the visible satellites and the stations.

In GNSS navigation and positioning, the so-called geometric accuracy factor DOP value is defined as a measure of the impact of satellite spatial geometric distribution on positioning accuracy. The cofactor matrix of unknown parameters is:

$$Q_{T_i} = \begin{bmatrix} q_{11} & q_{12} & q_{13} & q_{14} \\ q_{21} & q_{22} & q_{23} & q_{24} \\ q_{31} & q_{32} & q_{33} & q_{34} \\ q_{41} & q_{42} & q_{43} & q_{44} \end{bmatrix} \tag{15}$$

Each element in the formula reflects the precision information under the specific spatial geometric distribution of the satellite

Clock-difference precision factor

$$TDOP = \sqrt{q_{44}} \tag{16}$$

The corresponding median error of the clock difference is:

$$m_T = \sigma_0 \cdot TDOP \tag{17}$$

3D position accuracy factor:

$$PDOP = \sqrt{q_{11} + q_{22} + q_{33}} \tag{18}$$

Accuracy factors for combined impact:

$$GDOP = \sqrt{q_{11} + q_{22} + q_{33} + q_{44}} \tag{19}$$

Vertical component accuracy factor:

$$VDOP = \sqrt{q_{33}} \tag{20}$$

Level component accuracy factor:

$$HDOP = \sqrt{PDOP^2 - VDOP^2} \tag{21}$$

The ephemeris prediction taking into account the satellite occlusion condition can be obtained by the above steps.

4. BASELINE ESTIMATION OF VECTOR COFACTOR ARRAYS AND RDOP VALUES

In the traditional GNSS control network optimization design, most of them determine the weight of the baseline according to the nominal accuracy of the receiver, and this method does not relate to the actual observation conditions.

To ensure the accuracy of the measurement, the determination of the accuracy and weight of the baseline is an important link. According to the accuracy requirements of the control network, the synchronous observation baseline, the number of observation periods and the length of time period are reasonably selected to adjust the accuracy and weight of the baseline, so the designed observation scheme is closer to the actual. the estimation of the baseline relative positioning accuracy factor rdop value is introduced here. through the common satellite statistics, the double difference observation equation and the error equation are established. the relative positioning accuracy factor is determined according to the cofactor array of the parameters to be determined. Baseline endpoints, A (), B (), carrier phase observations at each station $x_1, y_1, z_1 x_2, y_2, z_2$ $\phi_i^j(t_1)$.

The double-differences of the observations are as follows:

$$\nabla \square \phi^k(t) = \left[\phi_2^k(t) - \phi_1^k(t)\right] - \left[\phi_2^j(t) - \phi_1^j(t)\right] \tag{22}$$

The pseudo-range observation equation is as follows:

$$\lambda \phi_i^j(t) = \rho_i^j(t) + c\left[\delta t_i(t) - \delta t^j(t)\right] - \lambda N_i^j(t_0) + \Delta_{i,I_p}^j(t) + \Delta_{i,T}^j(t) \tag{23}$$

For observational equations:

$$\lambda \varphi_i^j(t) = \rho_i^j(t) + c\delta t_i^j - \lambda N_i^j(t_0) + \Delta I_i^j(t) + \Delta T_i^j(t) \tag{24}$$

$\Delta I_i^j(t)$ $\Delta T_i^j(t)$ $\rho_i^j(t)$ and ionospheric and tropospheric errors, where the nonlinear term represents the geometric distance between the station and the satellite, respectively. The linearized carrier observation equation is:

$$\lambda \varphi_i^j(t) = (\rho_i^j(t))_0 - k_i^j(t)X_i - l_i^j(t)Y_i - m_i^j(t)\delta Z_i + c\delta t_i^j - \lambda N_i^j(t_0) + \Delta I_i^j(t) + \Delta T_i^j(t) \tag{25}$$

In the formula:

$$k_i^j(t) = \frac{1}{(\rho_i^j(t))_0}(X^j(t) - X_i^0)$$

$$l_i^j(t) = \frac{1}{(\rho_i^j(t))_0}(Y^j(t) - Y_i^0)$$

$$m_i^j(t) = \frac{1}{(\rho_i^j(t))_0}(Z^j(t) - Z_i^0)$$

The pseudo-range observation equation is:

$$P^j(t) = (\rho^j(t))_0 - k^j(t)X - l^j(t)Y - m^j(t)\delta Z + c\delta t^j + \Delta I^j(t) + \Delta T^j(t) \tag{26}$$

The double difference observation equation is as follows:

$$\begin{aligned}(P_2^j(t) - P_1^j(t)) - (P_2^i(t) - P_1^i(t)) &= -((k_2^j(t) - k_1^j(t)) - (k_2^i(t) - k_1^i(t)))\delta X \\ &-((l_2^j(t) - l_1^j(t)) - (l_2^i(t) - l_1^i(t)))\delta Y - ((m_2^j(t) - m_1^j(t)) - (m_2^i(t) - m_1^i(t)))\delta Z \\ &+(((\rho_2^j(t))_0 - (\rho_1^j(t))_0) - ((\rho_2^i(t))_0 - (\rho_1^i(t))_0))\end{aligned} \tag{27}$$

Observation equation:

$$V = AX + L \tag{28}$$

Of which:

$$V = \begin{bmatrix} (P_2^j(t) - P_1^j(t)) - (P_2^i(t) - P_1^i(t)) - (((\rho_2^j(t))_0 - (\rho_1^j(t))_0) - ((\rho_2^i(t))_0 - (\rho_1^i(t))_0)) \\ \vdots \\ (P_n^j(t) - P_1^j(t)) - (P_n^i(t) - P_1^i(t)) - (((\rho_n^j(t))_0 - (\rho_1^j(t))_0) - ((\rho_n^i(t))_0 - (\rho_1^i(t))_0)) \end{bmatrix}$$

$$A = \begin{bmatrix} -((k_2^j(t) - k_1^j(t)) - (k_2^i(t) - k_1^i(t))) & -((l_2^j(t) - l_1^j(t)) - (l_2^i(t) - l_1^i(t))) & -((m_2^j(t) - m_1^j(t)) - (m_2^i(t) - m_1^i(t))) \\ \vdots & \vdots & \vdots \\ -((k_n^j(t) - k_1^j(t)) - (k_n^i(t) - k_1^i(t))) & -((l_n^j(t) - l_1^j(t)) - (l_n^i(t) - l_1^i(t))) & -((m_n^j(t) - m_1^j(t)) - (m_n^i(t) - m_1^i(t))) \end{bmatrix}$$

by: $Q = (A^T PA)^{-1}$

Available Value: $RDOP$

$$RDOP = [tr(Q)]^{\frac{1}{2}} \tag{29}$$

Q According to The relative positioning accuracy factor of the baseline can be determined and the vector accuracy factor of the baseline can be decomposed into the form $RDOP(RDOP_{\Delta X}, RDOP_{\Delta Y}\ RDOP_{\Delta H})$.

At this point, you can based on the outline coordinates of the control network and the connection of the side length of the control network, the observation period plan is determined all baseline shared satellite and rdop values.

In addition, according to the study(Hao & Fang 2008)when the baseline common satellite is consistent with its endpoint visual satellite, the single point DOP value is consistent with the baseline RDOP value trend.

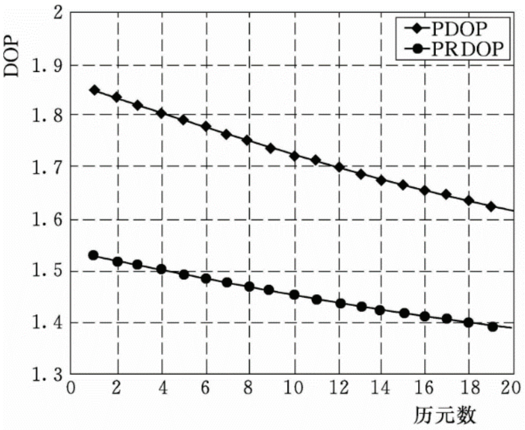

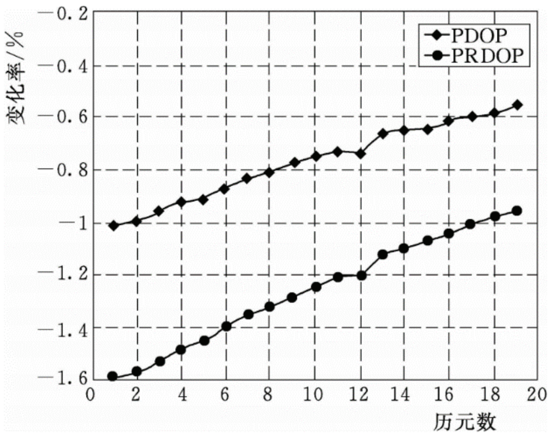

Figure 1 : Relationship between PDOP and RDOP **Figure 2** : Relationship between change rate of PDOP and RDOP.

It can be seen from figure 1 that its pdop is consistent with the rdop value result trend, and figure 2 shows that the rate of change between the two is also highly consistent, so it is also possible to evaluate the baseline dop value through the baseline common satellite condition and estimate the baseline rdop value accordingly. The results of the two assessment methods are consistent. All the key points need to be evaluated and analyzed first.

5. BASELINE SCREENING OF SYNCHRONOUS OBSERVATIONS BASED ON RDOP PRE-VALUATION

For the control network in the high mountain canyon, urban building group environment or replanted area, it is difficult to ensure the observation quality because of the barrier occlusion. In order to solve the problem of such control point observation difficulty, it is necessary to study the screening problem of the optimal observation baseline of the control point. The basic ideas are:

$(DOP_{\Delta X}, DOP_{\Delta Y}, DOP_{\Delta H})DOP$ Baseline relative positioning accuracy factor calculated. The simultaneous observation combinations of the target observation points are selected and the baselines of different observation periods are counted the observation accuracy of the synchronous ring is estimated according to the selected network conditions and the corresponding precision factors of the observation period.

Among them, the selection methods of synchronous observation points and observation periods are as follows:

Following the selection of the observation plan, statistical information such as common satellite visibility and DOP values for all baselines for multiple periods is given. Summarize the accuracy information of different time periods and different baselines.

Base line setting and combining according to the matching degree of DOP value in the same time period, and the optimal selection scheme (including the sequence of synchronous observation, the starting and ending time of the time period, the baseline information) is given as the basis for the selection evaluation of multiple schemes. Develop an observation plan.

DOP_d Difficulty in observing target points to establish a virtual synchronous observation relationship between the observed difficulty points and the n points of the constructable network to form each baseline Value DOP:

$$DOP_{d-1}, DOP_{d-2}, \ldots, DOP_{d-i}, \ldots DOP_{d-n}$$

DOP Yes The values are sorted in ascending order, and according to the number of instruments, R points are intercepted in order as the optimal synchronous observation baseline.

According to the above precision analysis results, combined with the site terrain and traffic conditions, can be the measurement control points of each synchronous observation period are determined under manual intervention.

The RDOP evaluation of a project control point A1 and A2- A12 is given below. The figure lists only the DOP values of the baseline of the control point A1 and the adjacent A10, A11, A12 and A2:

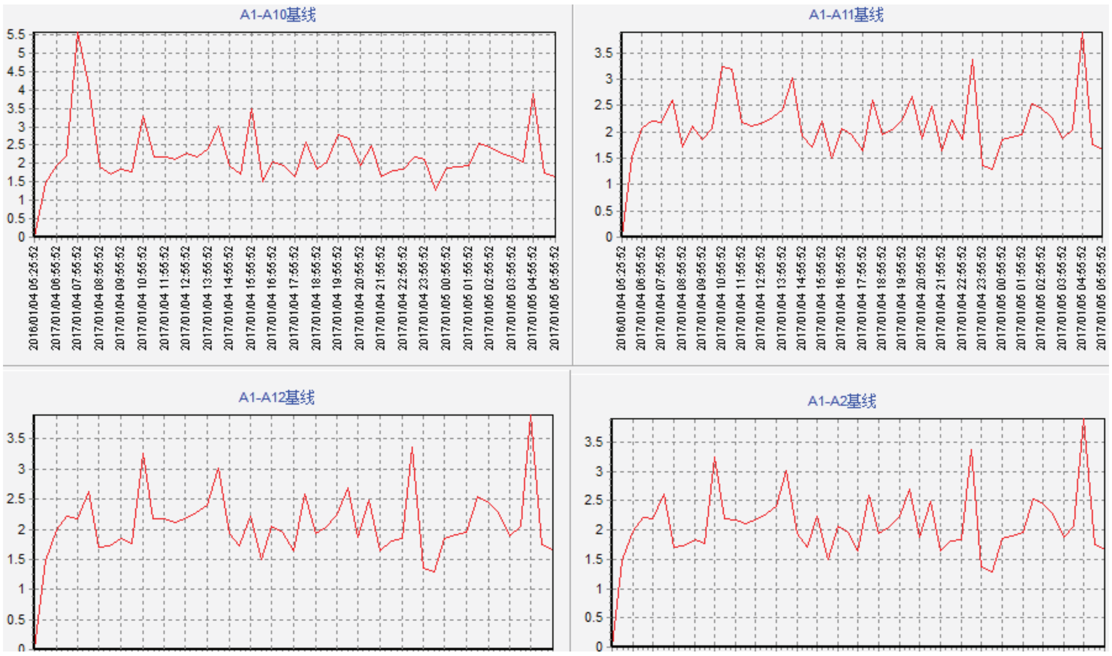

Figure 3 : Information of baseline RDOP values for simultaneous observation at point A1

According to the above information, it is easy to choose the most favorable observation combination among the alternative points, considering the network shape and traffic situation synthetically, right Multiple periods of observation Select evaluation, given Overall the preferred scheme (including synchronous observation order, time period start and end time, baseline information) to establish a favorable observation combination.

6. ACCURACY AND WEIGHT ESTIMATION OF BASELINE VECTORS

δ_R The accuracy of the control network can be estimated according to the network of the multiple synchronous rings determined above. The accuracy evaluation method adopts the variance matrix estimation algorithm of the common baseline vector. since the relative positioning accuracy factor index is provided in the estimate of the rdop value, and the point accuracy index based on it is dimensionless relative accuracy, the variance value determined by the nominal accuracy of the instrument is modified here with the estimated rdop value of 3.3.2 based on the method described in 2.4.1. Specific approaches are as follows:

If the nominal accuracy of the instrument is a + bppm and the baseline length is D, then the error in the baseline can be expressed as:

$$m_i = K\sqrt{a^2 + (b \times D_i)^2} \tag{30}$$

K_i in the formula for correction coefficients, the RDOP values and the empirical coefficients are evaluated Confirmed k_{exp}.

$$K_i = f(ki_{exp}, RDOP_i) \tag{31}$$

k_{exv} Experience factor and model selection, can be determined by historical data trial calculation, here can be taken multiplied by RDOP k_{exv}.

The right of adjustment is:

$$P_i = \frac{\delta_0^2 . n}{K_i^2 [a^2 + (b.D_i)^2]} \tag{32}$$

δ_0 In the formula for the unit weight median error and n for the number of baseline repeated measurements.

Each baseline variance matrix and weight matrix are thus identified. The method the evaluation accuracy is closer to the real situation, and it has obvious advantages in the optimization of the control network in the poor observation conditions.

m_i The accuracy of the above control points on the basis of the estimation, the theoretical design efficiency, practical design efficiency and total efficiency of the control network are further evaluated. Assessment of cost indicators using the size of the control network and the repeated station setting rate. Using the total number of independent baselines and the number of necessary baselines of the control network, the redundant baselines are evaluated, and the whole network reliability index and the net type precision benefit index are calculated. To evaluate the accuracy of each point in the current technical design scheme, as well as the accuracy of the side length of each baseline, the accuracy of the azimuth angle, the redundant observation components and other precision information, can obtain more in line with the actual situation information.

7. CONCLUSION

The paper studies the satellite visibility analysis, ephemeris prediction and precision evaluation method taking into account the condition of satellite occlusion boundary. On this basis, a baseline precision evaluation method and GNSS measurement based on the condition of space occlusion boundary are studied. control network accuracy estimation method.

R An ephemeris prediction method that takes into account the conditions of the satellite occlusion boundary. By establishing the constraint condition of the satellite occlusion boundary and combining with the satellite ephemeris, the satellite space position calculation and coordinate conversion are carried out at the ground station In the central coordinate system of the coordinate origin, the satellite visibility and satellite distribution in the selected period are analyzed, and then the precision factor evaluation of the single station is carried out according to the results of the satellite visibility analysis to provide more reliable ephemeris prediction information.

$[tr(Q)]RDOP$ GNSS measurement based on station-to-air occlusion boundary conditions Control network accuracy estimation method, using visible satellite as a constraint condition for baseline common satellite Analysis, establish double difference observation equation and error equation, according to the trace of the cofactor matrix of the undetermined parameter determination of the square root the relative positioning accuracy factor of the baseline, the simultaneous observation combination screening of the target observation points, and the statistics of each baseline in different observation periods The observation accuracy of the synchronous ring is estimated according to the selected network conditions and the corresponding precision factors of the observation period. The choice of time. The accuracy of the control network is estimated by using the variance matrix estimation algorithm of the baseline vector m_i.

The beneficial effects of this study are:

(1) Compared with the traditional method, it takes into account the actual visible satellite situation in the selected period of each target point in the accuracy assessment stage, and its single point DOP or estimated relative positioning accuracy factor has higher accuracy.

(2) This study is suitable for GNSS observation in high mountain canyon areas and difficult observation areas such as urban buildings environment. It can estimate the accuracy index which is highly consistent with the actual satellite receiving condition, draw up a more reliable observation plan according to the actual observation conditions, make a better observation dispatch plan according to the equipment and personnel conditions, and evaluate the accuracy index of the control network according to the established observation plan. For the high mountain canyon and urban buildings under the environment of GNSS observation program has an unprecedented advantage.

REFERENCES

Hao, X.G. & Fang, J. 2008. Research on density of the level ellipsoid. *Progress in Geophysics* 23(2): 392-397.

Hao, X.G., XU, H.Z. & Liu, D.J. 2001. A Preliminary Study of Mathematical Properties of the Parameter Ellipsoid. *Acta Geodaetica et Cartographica Sinica* 30(3): 203-207.

Li, H.P. & Bian, S.F. 2009. A Study of the Shape Difference between the Level Surfaces of the Oblate Spheroid and the Ellipsoid. *Acta Geodaetica et Cartographica Sinica* 38(2):95-100.

Yao, Y.B., Huang, C.M. & Li, C.C. 2012. A Mew Algorithem for Solution of Transformation Parameters of Big Rotation Angla's 3D Coordinate. *Geomatics and Information Science of Wuhan University* 3:253-256.

Wang, J.X. & Qiu, Y.Y. 2007. Influence of ellipsoidal height error on seven-parameter transformation. *Journal of Geodesy and Eodynamics* 27(2):25.

Du, X.F. Zhang, X.F. & Jiang, L.L. 2009. A method of GPS net adjustment for big rotating angel. *Science of Surveying and Mapping* 34(4): 88-89.

Shi, K., Chen, Y.B., Chen, Y.G., Ding, R.J. & Zi, C.B. 2004. A New approach to the translation computations between ellipsoid and gauss projection plane with variable size parameter of Ellipsoid. *Journal of Kunming University of Science and Technology* 29(5): 1-5.

Niu, Z.L. & Lai, C.Y. 1998. Discussion of Question for Establishing Regional Coordinate System. *Engineering of Surveying and Mapping* 4: 13-16+21.

Li, Z.F., Zhao, Y.H. & Ju, T.L. 2010. Limitation of GPS integrated projection algorithm for weighted scale than on a side. *Engineering Investigation* 2: 75-78.

Shi, Y.M. & Zhang, W.Q. 2000. The optimal determination of the regional ellipsoid elements. *Engineering of Surveying and Mapping* 3:27-29+40.

Cao, X.Y., Wang, J. & Liu, C. 2013. Analysis of availability of dop to forecast GNSS relative positioning. *Journal of Geodesy and Geodynamics* 01: 81-85.

Fund project: China Power Construction Group Northwest Survey and Design Institute Limited Technology Projects (Item No. XBY-2016-10)

China Hydropower Engineering Consultants Group Science and Technology Project (Project No. GW-KJ-2012-21).